

# Fuel Efficient Computation in Passive Self-Assembly

Robert Schweller\*

Michael Sherman†

## Abstract

In this paper we show that passive self-assembly in the context of the tile self-assembly model is capable of performing fuel efficient, universal computation. The tile self-assembly model is a premiere model of self-assembly in which particles are modeled by four-sided squares with glue types assigned to each tile edge. The assembly process is driven by positive and negative force interactions between glue types, allowing for tile assemblies floating in the plane to combine and break apart over time. We refer to this type of assembly model as passive in that the constituent parts remain unchanged throughout the assembly process regardless of their interactions. A computationally universal system is said to be fuel efficient if the number of tiles used up per computation step is bounded by a constant. Work within this model has shown how fuel guzzling tile systems can perform universal computation with only positive strength glue interactions [33]. Recent work has introduced space-efficient, fuel-guzzling universal computation with the addition of negative glue interactions and the use of a powerful non-diagonal class of glue interactions [20]. Other recent work has shown how to achieve fuel efficient computation [28] within active tile self-assembly. In this paper we utilize negative interactions in the tile self-assembly model to achieve the first computationally universal passive tile self-assembly system that is both space and fuel-efficient. In addition, we achieve this result using a limited diagonal class of glue interactions.

## 1 Introduction

Self-assembly is the process by which systems of simple objects organize themselves through local interactions into larger, more complex objects. There are

perhaps two categories of self-assembly: passive and active. In passive self-assembly the objects of the system are simple, stagnant particles that interact simply by surface chemistry and geometry. In contrast, objects within an active self-assembly model may be permitted to move, rotate, adjust state, or add and remove bonding domains based on local interactions. Put another way, active self-assembly extends traditional passive self-assembly by considering the objects of the system to be simple robots with abilities that vary according to the particular model considered.

The study of passive self-assembly is important for multiple reasons. First, many theoretical models of active self-assembly do not currently have satisfactory implementations at the nanoscale. In contrast, many computationally interesting passive tile self-assembly constructions are seeing experimental success based on DNA implementations [7, 24, 30]. Further, it is plausible that many active self-assembly models will see implementation through constructions built up within passive self-assembly models. For example, the system proposed in this paper which implements a space-efficient, fuel-efficient universal computation system might be modified to serve as the internal machinery for a larger, active component, thus potentially allowing for a passive self-assembly system to simulate the behavior of a more powerful active system. Finally, it is important to understand the power and limits of passive self-assembly to better understand when active components are truly necessary.

In this paper we focus on an established model of passive self-assembly, the tile assembly model (TAM). Monomers in the TAM are unit squares with glue types assigned to edges. Self-assembly is driven by a large (infinite) number of copies of a set of tile types floating about, bumping into one another in the plane, and potentially sticking together when glue affinities exceed some set threshold. While simple, the TAM has been extensively studied [1–6, 8–14, 16–19, 22, 23, 25–27, 31, 32] and shown to be capable of universal computation [33], and even recently shown to be intrinsically universal [21] in the case of the *abstract* TAM.

\*Department of Computer Science, University of Texas - Pan American, [rtschweller@utpa.edu](mailto:rtschweller@utpa.edu) This author's research was supported in part by National Science Foundation Grant CCF-1117672.

†Department of Computer Science, University of Texas - Pan American, [mjsherman@utpa.edu](mailto:mjsherman@utpa.edu) This author's research was supported in part by National Science Foundation Grant CCF-1117672.

Within the TAM, we consider the problem of improving existing universal computation results by obtaining *fuel-efficiency*. A TAM system that simulates a Turing machine is said to be fuel-efficient if only a constant number of tiles are used up per computation step. This requirement, or close approximations to it, are of fundamental importance for the implementation of scalable molecular computers. Unfortunately, all passive variants of the TAM have failed to yield fuel-efficient universal computation.

To address this *fuel-deficiency*, we consider the TAM with the added power of negative glue interactions. The power of negative force interactions stems from the possibility of stable assemblies coming together with strong affinities and yet producing unstable products that subsequently break apart into pieces that are different from the original pair of assemblies. By careful engineering, this property can be harnessed to allow assemblies to attach to specific locations of large assemblies, surgically pry off and replace small portions of the assembly, and finally detach the replacement mechanism and repeat the process. If you imagine that the large assembly represents the tape of a Turing machine, and that the location of attachment occurs at the current head location of the machine, you get a high level overview of our Turing machine simulation that only uses up a fixed number of tile types per computation step. This stands in contrast to previous fuel-guzzling work in which each computation step is simulated by the assembly of a complete, slightly modified, copy of the entire tape.

**1.1 Related Work** Doty et. al. [20] first considered the effect of negative interactions in self-assembly and showed how to design space-efficient computational self-assembly systems by utilizing negative glues to slice off a previous assembly state after computing the next state. This state transition construction can be applied to the simulation of a Turing machine. However, their construction does not achieve fuel efficiency in that each computational step uses up a number of tiles on the order of the current size of the tape. Their result is also not applicable to our graph traversal system in that their technique, modified to the graph traversal problem, would lead to dead end assemblies that violate the required dynamics of the graph traversal. Finally, their paper utilizes a very powerful *non-diagonal* version of the tile self-assembly glue function. We restrict ourselves to the much more restricted diagonal class of glue functions in which glues may only interact with

similarly labeled glues. Also, this restricted diagonal class of glue functions allows us to maintain a strict separation between positive and negative glues which is likely more feasible for experimental implementation. Additionally, Doty et. al. provide an elegant amortized analysis proof showing a limit to the extent to which tile reuse can be achieved with negative force interactions within the TAM. We implicitly use their result in that it allows us to reasonably simplify our definition of fuel usage to not deal with tile reuse.

Some recent work has been done that shows provable increases in power of active self-assembly systems over passive TAM systems. Recent work by Woods et. al. [34] and Nadine Dabby and Ho-Lin Chen [15] has shown that local rule based active self-assembly systems are able to assemble large shapes in poly-logarithmic time when the monomers of the system are able to perform operations such as pushing a row of placed monomers a unit of distance in some direction. Another recent work by Padilla et. al. [28] considers an active tile self-assembly model motivated by a DNA strand replacement mechanism in which tiles can pass simple, fire-once signals from one tile edge to another. They show that this simple mechanism allows for the implementation of fuel-efficient universal computation, as well as additional efficiencies that are provably impossible within the passive TAM.

Additional investigations have looked into self-assembly models that allow self-assembly detachment, a key requirement for the implementation of space-efficient computations [1, 6, 25, 32]. Other recent work has considered negative glues within the TAM to achieve universal computation with a very limited set of glues at temperature-1 [29].

**Paper layout.** In Section 2 we define the tile assembly model and present definitions that define our graph traversal and Turing machine simulation problems. In Section 3 we present our construction for fuel efficient graph walking. In Section 4 we present a simple example graph walking system that implements a base-4 oscillator. In Section 5, we extend our graph walking construction to simulate Turing machines. Finally, in Section 6 we conclude with a discussion of future research directions.

## 2 Definitions and Model

In this section we first define the two-handed tile self-assembly model with both negative and positive strength glue types and diagonal glue functions. We also formulate the problem of designing a tile assembly system that walks a given input graph, as

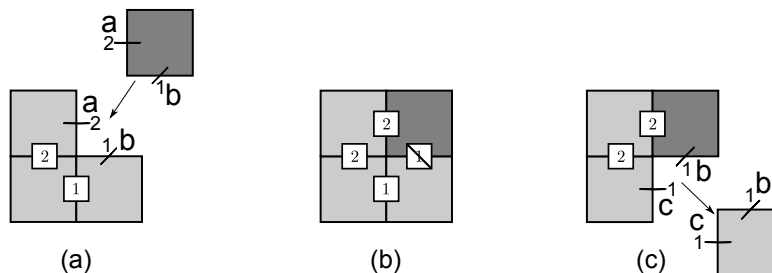


Figure 1: This figure introduces our notation for our constructions, as well as a simple example of combination and detachment events. We denote positive glues with vertical and horizontal lines protruding from tile edges along with numbers and labels denoting glue strength and type. Negative strength glues are labeled with slanted lines. Finally, bonded glues between adjacent tiles are depicted with a number denoting the bond strength inscribed within a box between the bonded tile edges. (a) The 3-tile assembly on the left and the singleton gray tile are combinable into a  $2 \times 2$  square shown in (b) as the cut between the 2 assemblies yields strength 1. Note, however, that the producible  $2 \times 2$  square in (b) is not stable and is breakable into the assemblies shown in (c).

well as the concept of fuel efficiency.

### 2.1 Tile Self-Assembly Model

**Tiles.** Consider some alphabet of glue types  $\Pi$ . A tile is a finite edge polygon with some finite subset of border points each assigned some glue type from  $\Pi$ . Further, each glue type  $g \in \Pi$  has some rational number strength  $str(g)$ . Finally, each tile may be assigned a finite length string *label*. In this paper we consider a special class of tiles that are unit squares of the same orientation with at most one glue type per face, with each glue being placed exactly in the center of the tile's face.

**Assemblies.** An assembly is a set of tiles whose interiors do not overlap. For a given assembly  $\Upsilon$ , define the *bond graph*  $G_\Upsilon$  to be the weighted graph in which each element of  $\Upsilon$  is a vertex, and each edge weight between tiles is the sum of the strengths of the overlapping, matching glue points of the two tiles. An assembly  $C$  is said to be *stable* if the bond graph  $G_C$  has min-cut at least 1, and *unstable* if the min-cut is less than 1. Note that if the set of border points of all tiles in an assembly is not a connected set, then the assembly cannot be stable. Note that only overlapping glues that are the same type contribute a non-zero weight, whereas overlapping, non-equal glues always contribute zero weight to the bond graph. The property that only equal glue types interact with each other is referred to as the *diagonal glue function* property and is perhaps more feasible for experimental implementation than more general glue functions. Additionally, with the square tiles considered in this paper, stable

assemblies will necessarily consist of tiles stacked face to face, forming a subset of the 2D grid.

For an assembly  $A$ , let  $A^*$  denote the set of all assemblies that are equal to  $A$  up to translation. For a set of assemblies  $T$ , let  $T^*$  denote the set of all assembly sets  $A^*$  such that  $A \in T$ . Put another way,  $T^*$  is a set that represents a set of assemblies  $T$  if we do not care about translation.

**Breakable Assemblies.** For an (unstable) assembly  $C$  whose bond graph  $G_C$  has a cut into assemblies  $A$  and  $B$  with weight less than 1, we say that  $C$  is *breakable* into  $A$  and  $B$ .

**Combinable Assemblies.** Informally, two assemblies  $A$  and  $B$  are said to be combinable into an assembly  $C$  if the assemblies can be translated together in such a way that they do not overlap and the sum of the matched glue strengths between the two assemblies is at least 1. Formally, consider two assemblies  $A$  and  $B$ . If  $B$  can be translated into  $B'$  such that  $C = A \cup B'$  is a valid (not overlapping) assembly such that the cut of  $G_{A \cup B'}$  into  $A$  and  $B'$  has strength at least 1, then we say that  $A$  and  $B$  are *combinable* into  $C$ .

Note that  $A$  and  $B$  may be combinable into an assembly that is not stable. This is a key property that is leveraged throughout our constructions. See Figure 1 for an example.

**Producible Assemblies.** A set of initial assemblies  $T$  has an associated set of *producible* assemblies,  $PROD_T$ , which define what assemblies can grow from the initial set  $T$  by any sequence of combination and break events. Formally,  $T \subseteq PROD_T$  as a base case set of producible assemblies. Further, given

any  $A, B \in \text{PROD}_T$  with  $A$  and  $B$  combinable into  $C$ , then  $C \in \text{PROD}_T$ , and for any  $C \in \text{PROD}_T$  where  $C$  is breakable into  $A$  and  $B$ , then  $A, B \in \text{PROD}_T$ . Put another way, the set of producible assemblies contains any assembly that can be obtained by a valid sequence of combinations and breaks, starting from the initial set of assemblies  $T$ . We further define the set of *terminal* assemblies,  $\text{TERM}_T$ , to be the subset of  $\text{PROD}_T$  such that no element of  $\text{TERM}_T$  can undergo a break or combination transition with another element of  $\text{PROD}_T$ .

Typically, we require that an initial assembly set consist only of stable assemblies. When  $T$  consists only of assemblies that are singleton tiles,  $T$  is called a *tile set*.

## 2.2 Additional Definitions

**Valid Assembly Sequence.** For an initial assembly set  $T$ , a valid assembly sequence for  $T$  is any sequence of assemblies  $S = \langle a_1, \dots, a_k \rangle$  such that each  $a_i \in \text{PROD}_T$ , and for each  $i$  from 1 to  $k-1$ ,  $a_i$  is either combinable with some  $b \in \text{PROD}_T$  to form  $a_{i+1}$ , or  $a_i$  is breakable into  $a_{i+1}$  and  $b$  for some assembly  $b$ . In addition, a valid assembly sequence  $S$  is said to be  $\ell$ -*focused* for label  $\ell$  if each assembly in  $S$  contains at least one tile with label  $\ell$ . A valid assembly sequence is said to be *nascent* if  $a_1 \in T$ .

For a given partial function  $f : \text{PROD}_T \rightarrow V$  for a set  $V$ , define function  $f'(\langle a_1, \dots, a_k \rangle)$  to be a function from assembly sequences over  $\text{PROD}_T$  to sequences over  $V$  defined by replacing each  $a_i$  with  $f(a_i)$  if  $f(a_i)$  is defined, and deleting  $a_i$  if  $f(a_i)$  is not defined.

**Graph Walking Assemblies.** Consider a directed graph  $G = (V, E)$ , a start vertex  $s \in V$ , and an initial assembly set  $T$  in which some tiles of some assemblies are labeled with  $\ell$ .  $T$  is said to *walk* graph  $G$  if there exists a partial function  $f : \text{PROD}_T \rightarrow V$  such that:

1. (assembly sequences are walks) For any  $\ell$ -focused nascent assembly sequence  $S$  of  $T$ ,  $f'(S)$  is a valid walk of  $G$  starting at vertex  $s$ .
2. (walks are assembly sequences) For any walk  $W$  of  $G$  starting at vertex  $s$ , there exists a nascent,  $\ell$ -focused assembly sequence  $S$  such that  $f'(S) = W$ .
3. (no undesired dead-ends) Consider an edge  $(u, v) \in E$ . Then for any  $\ell$ -focused assembly sequence  $S$  such that  $f'(S) = \langle u \rangle$ , there exists an  $\ell$ -focused assembly sequence  $R$  such that  $S$  is a prefix of  $R$  and  $f'(R) = \langle u, v \rangle$ .

In this definition, the  $\ell$  label is meant to denote tiles and assemblies that are meant to be part of the output, and not garbage. That is, to walk a graph efficiently there will necessarily be dead-end garbage assemblies. Our definition thus requires that all such garbage assemblies be free of the  $\ell$  label and thus can be distinguished from the assemblies that represent the graph walking assemblies. In a sense, our definition states that if you stare at one  $\ell$ -labeled tile within an assembly, over time the assembly containing that tile will be guaranteed to walk the graph correctly, whereas if you stare at a portion of the assembly that is not labeled with the  $\ell$ , it is possible that portion may detach and become garbage at some point.

**Fuel Efficiency.** Consider two assemblies  $a$  and  $b$ . Define  $\text{fuel}(a, b)$  to be  $|b| - |a|$  if  $|b| \geq |a|$ , and zero otherwise. For an assembly sequence  $A = \langle a_1, \dots, a_k \rangle$ , define  $\text{fuel}(A)$  to be  $\sum \text{fuel}(a_i, a_{i+1})$ .

For a tile set  $T$  that walks a directed graph  $G$ ,  $T$  is said to be *fuel efficient* if for all  $\ell$ -focused, nascent assembly sequences  $S$ ,  $\text{fuel}(S)/|f'(S)| = O(1)$ . That is, for all possible walks, the average fuel per vertex transition is bounded by a constant.

## 3 Graph Walking

In this section we construct a tile assembly set for the fuel-efficient walk of a given input directed graph:

**THEOREM 3.1.** *For any given finite directed graph  $G = (V, E)$ , there exists a fuel efficient initial assembly set  $T$  that walks  $G$ . Further,  $T$  contains at most  $O(|V| + |E|)$  distinct assemblies each of  $O(1)$  size.*

This theorem can be slightly strengthened in that it is possible to modify the construction so that  $T$  consists of only singleton tiles. However, for clarity we do not present this modification.

The construction for this result serves two purposes. First, we believe the result itself is interesting. One example corollary is the ability to implement oscillator self-assembly systems with an example given in Section 4. The second purpose is that this construction presents some of the key techniques in a simplified form that we will extend to construct our main result: fuel efficient Turing machines.

The remainder of this section describes the construction for the proof of this theorem.

**3.1 Template Assembly Set** The following tile assembly template allows one to create an assembly set that can non-deterministically walk across a di-

rected graph. This template creates an assembly set that has  $O(|V| + |E|)$  assembly types. Also, the template uses a modest 9 fuel tiles per transition step. An example of constructing an assembly set using this template follows in Section 4 where we build a base four oscillator.

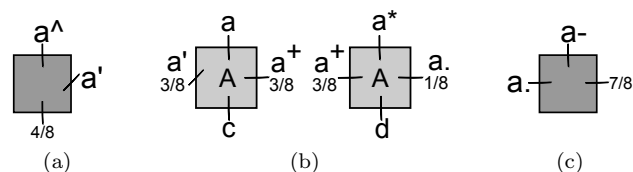


Figure 2: These four tiles are needed in order to represent a vertex in a graph. All glues labeled with some form of an  $a$  require unique glues to the specific vertex these tiles represent and may not be shared amongst other vertices. The tile in Figure 2a allows an edge gadget to detach its corresponding vertex. The tile in Figure 2c allows an edge gadget to know when its vertex has finished attaching. Finally, the pair of tiles in Figure 2b represent a single vertex in a graph.

**Vertex Representation.** For each vertex in the graph you must have the set of two tiles shown in Figure 2b, a vertex detachment tile shown in Figure 2a, and finally a vertex attachment tile which is shown in Figure 2c. The five glues labeled  $a'$ ,  $a^*$ ,  $a^-$ ,  $a^+$  and  $a$  on the duple of Figure 2b are unique to some vertex  $a$  while the two southern glues are the same for all pairs of tiles.

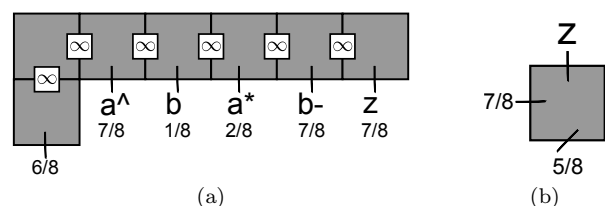


Figure 3: The edge gadget and its detachment tile. The assembly in Figure 3a is the edge gadget and represents a directed edge from vertex  $a$  to vertex  $b$ . The tile in Figure 3b is the tile that will allow the edge gadget to detach itself once done.

**Edge Gadget.** Figure 3a is the edge gadget which exchanges a vertex  $a$  with the vertex  $b$  on the cell assembly. When the edge gadget detaches itself from the cell assembly all tiles that detach with the gadget are no longer usable. In Figure 3a the glues

labeled with some  $a$  represent glues unique to some vertex  $a$  while the glues labeled with some  $b$  represent glues specific to some vertex  $b$ . The glue labeled with a  $z$  is unique to the edge detachment tile shown in Figure 3b. This tile allows the edge gadget including its junk to detach from the cell assembly.

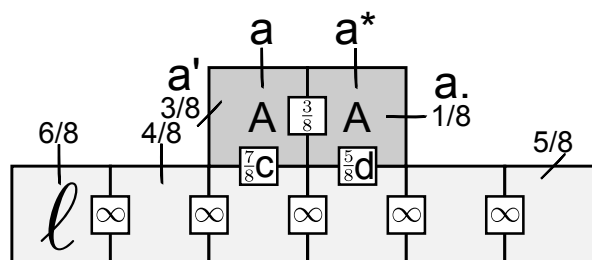


Figure 4: The initial pre-built starting cell assembly with a vertex already attached. As can be seen in the figure, we have labeled one of the tiles on the cell with an  $\ell$  making any assembly sequence which contains it  $\ell$ -focused.

**Cell Assembly.** This cell assembly is assumed to be pre-built and contains the initial starting vertex  $v$  already placed on top of the cell assembly. As you can see in Figure 4 the glues  $c$  and  $d$  are not discriminatory and allow any two tiles representing a vertex to attach to the cell assembly with the aid of an edge gadget. The  $\frac{6}{8}$ <sup>th</sup> glue along with the  $a^*$  glue allow the edge gadget to attach. After the attachment the  $\frac{4}{8}$ <sup>th</sup> glue allows for the widget to get a better “grip” on the assembly cell so that it may detach the current vertex. The final  $\frac{5}{8}$ <sup>th</sup> glue on the assembly allows the edge gadget to pry itself off.

**3.2 Correctness** As can be seen from Figure 5 the possible transitions made by changing from one state to another are straight forward and verifying that each single tile addition must happen in the order shown is left as a short exercise to the reader. We will concentrate on the two negative glue detachment events which are more complex and need to be verified so as to ensure that no other cuts in the produced assemblies are unstable other than those depicted. We shall assume that each vertical column of the image represents a stage in the transition and so there are a total of 9 stages from start to finish.

**Correct Gadget Removal.** After the gadget is done a tile may attach to the negative  $\frac{5}{8}$ <sup>th</sup> glue on the cell assembly which in turn pops off the edge gadget along with any junk. Two scenarios are brought about by the infinite binding within the cell assembly

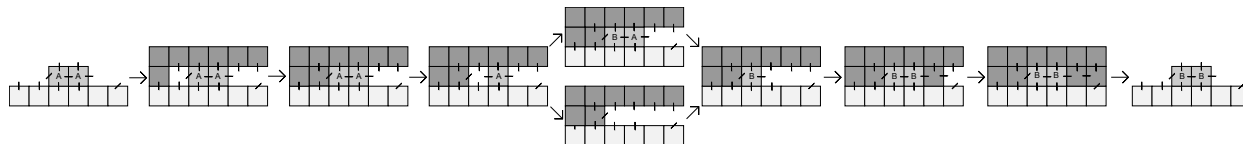


Figure 5: The steps necessary to transition from one state to another.

and edge gadget independently. The first scenario occurs when the cell assembly and edge gadget end up on opposite sides of the detachment. The other happens when both the cell assembly and edge gadget end up on the same side of the detachment. We will analyze both of these scenarios and show that from stage 8 in Figure 5 the only valid detachment is what results in stage 9.

Suppose both the cell and the gadget detach to opposite sides of the cut. We must include a negative glue to get an unstable cut and so the edge detachment tile must be on the same side as the gadget. This gives us a cut with weight  $\frac{1}{8}$  not taking into account any of the other four labeled tiles. For the cut to be unstable we can only increase the weight by  $\frac{6}{8}$  so as to keep it below 1. To stay unstable both the vertex detachment tile and the vertex attached tile must be on the side of the edge gadget because of their  $\frac{7}{8}$  attachment. Also, the left vertex tile must stay on the side of the cell assembly for the same reason. With this new information the total weight of the cut is now  $\frac{6}{8}$  and we only have the right vertex tile to place. The right vertex tile must now stay on the side of the cell because to keep the cut unstable we may only increase the weight of the cut by  $\frac{1}{8}$  more. Therefore, it is easy to see that the only possible unstable cut if both the cell and gadget are on opposite sides is the one displayed in Figure 5.

Now, suppose that both the cell assembly and the edge gadget detach to the same side of the cut. In order to include the negative strength of the edge detachment tile it must be on the opposite side of both the edge and the gadget. This immediately shows us that our cut is  $\frac{9}{8}$  which is stable. With no other negative glue interactions, there is no cut with both the cell assembly and the edge gadget on the same side that would lead to a detachment.

Therefore, since we have exhaustively explored both scenarios using the fact that the cell assembly and edge gadget are infinitely bound we can say that the only unstable cut at stage 8 is the one that results in stage 9.

**Correct Vertex Replacement.** Assume we are in stage 3 of Figure 5. We will show that the

transition to stage 4 is the only valid detachment event that may happen. If the cell and edge gadget were to detach to opposite sides of the cut this would give us a cut with weight  $\frac{5}{8}$ . Then, no matter which side of the cut you place the vertex removal tile all cuts will be above 1. If both the edge gadget and the cell are on the same side of the cut, the left vertex tile must be on the opposite side of the cut since the vertex removal tile will not fall out. This means that either the left vertex tile or both vertex tiles must be on the opposite side of the cut. If both vertex tiles are on the opposite side of the cut we have a cut with weight  $\frac{11}{8}$  which is stable. On the other hand, if it is only the left vertex tile on the opposite side of the cut then the weight of the cut is  $\frac{7}{8}$  which enables it to detach. Therefore, the only detachment event that can occur after stage 3 is the single left vertex tile detaching from the assembly leaving the assembly in stage 4. Once in stage 4 the right vertex tile destabilizes and may detach, leaving room for the next vertex to attach and stage 6 to come about.

#### 4 Quaternary Oscillator

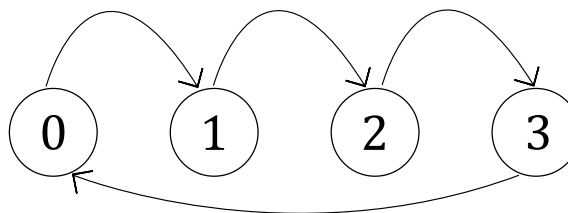


Figure 6: The directed graph of a quaternary oscillator.

A quaternary oscillator can be drawn as a directed graph with vertices representing each digit in the base-4 numeral system and the directed edges marking the transition from one numeral to the next. Figure 6 shows a directed graph representing a quaternary oscillator. The Graph Walking Template Assembly Set from Figures 2, 3, and 4 is non-deterministic when any vertex in the graph has more than one outgoing edge because any one of the edges

may attach and continue to transition. The quaternary oscillator in Figure 6, on the other hand, has only a single outgoing edge for any vertex making the template deterministic. Figure 7 represents the complete assembly set necessary to represent the graph in Figure 6. This is a straightforward example of how to create a concrete assembly set using the assembly template presented in Section 3.1.

### 5 Fuel Efficient Universal Computation

In this section we describe how to construct an initial assembly set  $T$  that will simulate a given Turing machine  $M$ . To formally define simulation of a Turing machine, we utilize our graph walking formulation. For a given Turing machine  $M$ , we consider all possible tape configurations, states, and head locations the machine may enter over time and form a directed graph over these possible configurations depicting which configurations the machine may transition between within a single computation step. With this definition we say that an assembly set  $T$  simulates  $M$  if it walks this configuration graph.

Formally, we define the simulation as follows:

**Turing Machine Simulation.** Consider some Turing Machine  $M = \langle Q, \Gamma, b, \Sigma, \delta, q_0, F \rangle$ , an initial tape  $t$ , and head position  $h$ . Let a possible *status* of  $M$  be a 3-tuple  $S = \langle \text{state}, \text{tape}, \text{head} \rangle$  where **state** represents some current state from  $Q$ , **tape** is some string of symbols over  $\Gamma$ , and **head** specifies a location on the tape where the Turing machine head currently sits. Additionally define the *start* status for a Turing machine  $M$  and an input tape  $r$  as the status corresponding to **tape** =  $r$ , **head** =  $h$ , and **state** =  $q_0$ .

Given a Turing machine  $M$ , define a directed graph  $G_M$  where the set of all statuses for  $M$  are vertices, and there exists an edge from any status  $a$  to status  $b$  if and only if  $M$  can transition from status  $a$  to  $b$  in one step. Finally, we say an initial assembly set  $T$  *simulates* Turing machine  $M$  if  $T$  walks  $G_M$ . Further, we say  $T$  is a *fuel-efficient* simulation of  $M$  if  $T$  constitutes a fuel-efficient walk of  $G_M$ .

Our main result is as follows:

**THEOREM 5.1.** *For any Turing machine  $M$ , there exists an initial assembly set  $T$  such that  $T$  is a fuel-efficient simulation of  $M$ . Further,  $|T| = O(|\Gamma| \cdot |Q|)$ , and each element of  $T$  is of  $O(1)$  size.*

As with our graph walking theorem, it is possible to strengthen this theorem such that  $T$  contains only singleton tile assemblies. For clarity of presentation and space, we omit the extended construction that

achieves this.

The remainder of this section presents the construction that proves Theorem 5.1

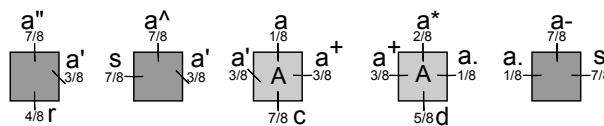


Figure 8: These tiles represent a symbol and state pair along with their needed utility tiles.

#### 5.1 Template Tile Set

**Symbols And States.** For our construction we add an additional state, the empty state  $\emptyset$ , to  $M$  which will be used to represent a symbol with no state i.e. a location where the head of the Turing Machine currently is not. For every symbol in  $\Gamma$  and every state in  $Q$  including  $\emptyset$  we create the set of tiles shown in Figure 8. This means that we should have exactly  $|\Gamma| \cdot (|Q| + 1)$  sets of tiles. The two center tiles labeled with an  $A$  in Figure 8 will represent some duple  $(a \in Q, s \in \Gamma \cup \emptyset)$ . We define a stateless state symbol pair as having the  $\emptyset$  state while a stateful state symbol pair has some  $q \in Q$ . The two leftmost tiles are called state symbol detachment tiles and detach the particular state symbol tile pair they were created with. This will be useful later when trying to transition the state of the Turing Machine. Finally, the last tile on the right is the state symbol attached tile and will allow the assemblies to know that the state symbol tile pair associated with it have both been attached.

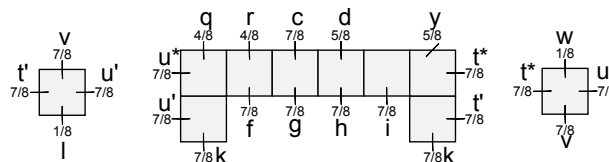


Figure 9: This assembly represents a single position on the tape. It is a tape cell which can and should contain some symbol state pair atop it attached to glues  $c$  and  $d$ . The two accompanying tiles are what will allow the tape to extend to the right or left.

**Tape Cell.** A tape cell in our construction is a single piece of tape which contains some state symbol tile pair taken from Figure 8. If the state contained on the tape cell is  $\emptyset$  then the tape cell contains only data, i.e. a symbol from  $\Gamma$ . On the other hand, if the

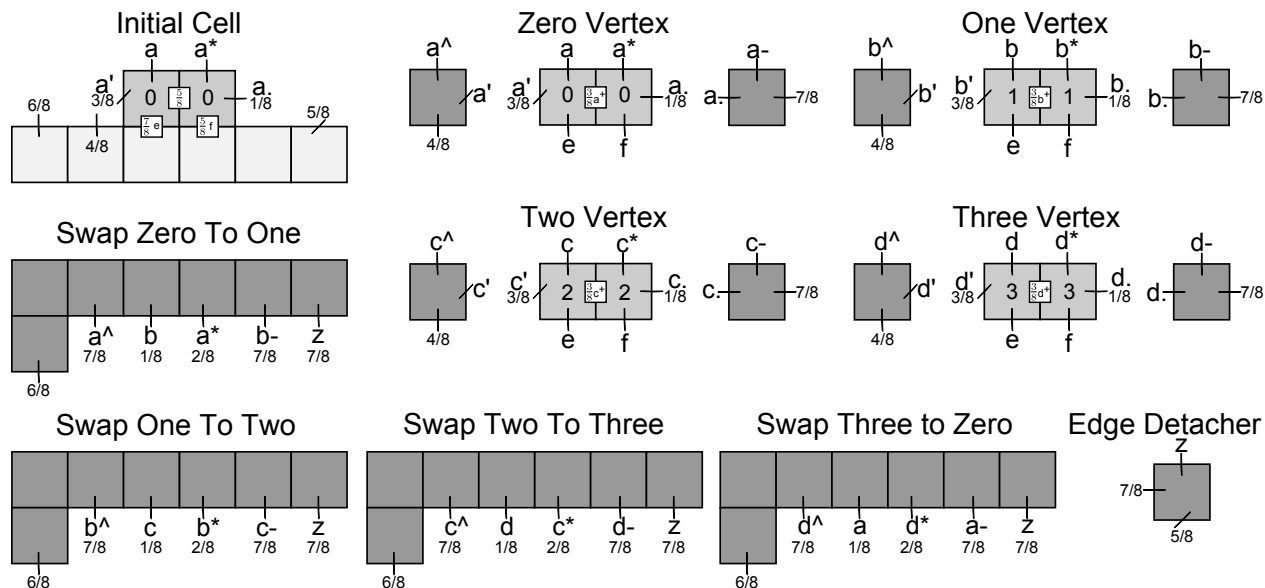


Figure 7: The complete assembly set for creating a quaternary oscillator.

state contained on the tape is not  $\emptyset$  then the location of the Turing Machine's head is at that location and it contains some symbol from  $\Gamma$ . The whole of the tape is then at least one tape cell possibly combined with many more tape cells attached together with the head of the tape in only a single location i.e. with a single cell containing a state unequal to  $\emptyset$  at any given time. Should the head of the Turing Machine be placed in multiple locations it will result in undefined behavior. When we later extend the tape we insure that the extended piece of tape gets initialized automatically to the blank state; i.e. the symbol  $b$  in combination with the state  $\emptyset$ . It is important to note that in order to properly transition across the directed graph  $G_M$ , we must label a tile on the left-most starting tape cell with an  $\ell$ .

**Transition Function.** A Turing Instruction is the 5-tuple  $I = \langle c \in Q, s \in \Gamma, p \in \Gamma, \{L, R\}, n \in Q \rangle$  where  $c$  is the current state,  $s$  is the scanned symbol,  $p$  is the symbol to print,  $\{L, R\}$  is the left or right movement of the head, and  $n$  is the new state. For each Turing Instruction in  $M$  create  $|\Gamma|$  transition gadgets. A single transition gadget is shown in Figure 10.

For two state symbol pairs we follow the same process as exchanging a single vertex in the Graph Walking Template with a few exceptions. The most obvious exception is that we are now exchanging two symbol state pairs instead of a single vertex pair. In order to facilitate this change we extend the

transition gadget to accompany the two exchanges. The next difference is that after exchanging the first pair of tiles the next symbol state pair must be exchanged instead of detaching the whole transition gadget. This is the reason for needing two state symbol detachment tiles instead of just the single one as in the Graph Walking Template. Now, of the two detachment tiles the first is used when detaching the left state symbol pair underneath the transition gadget and the second is used when detaching the right state symbol pair underneath the transition gadget. This along with the changing of a couple glue strengths gives us a transition gadget shown in Figure 10 that is able to exchange two symbol state pairs at the same time.

Now, in order to create the transition gadgets which represents a Turing instruction, we must properly set the label of several unlabeled glues. We will temporarily number the unlabeled glues in Figure 10 from 1 starting at the left to 8 at the farthest right. It does not matter whether you are moving the head left or right, the stateful pair always becomes stateless and the stateless pair always becomes stateful. Therefore, the only difference between moving the head right or left is that the stateful pair is at the left when moving right or at the right when moving left. We will continue to assume that we are creating the transition gadgets for some  $I$  which moves the head to the right. Since we are moving right, glues 3 and 1 will use the proper glue labels for the state





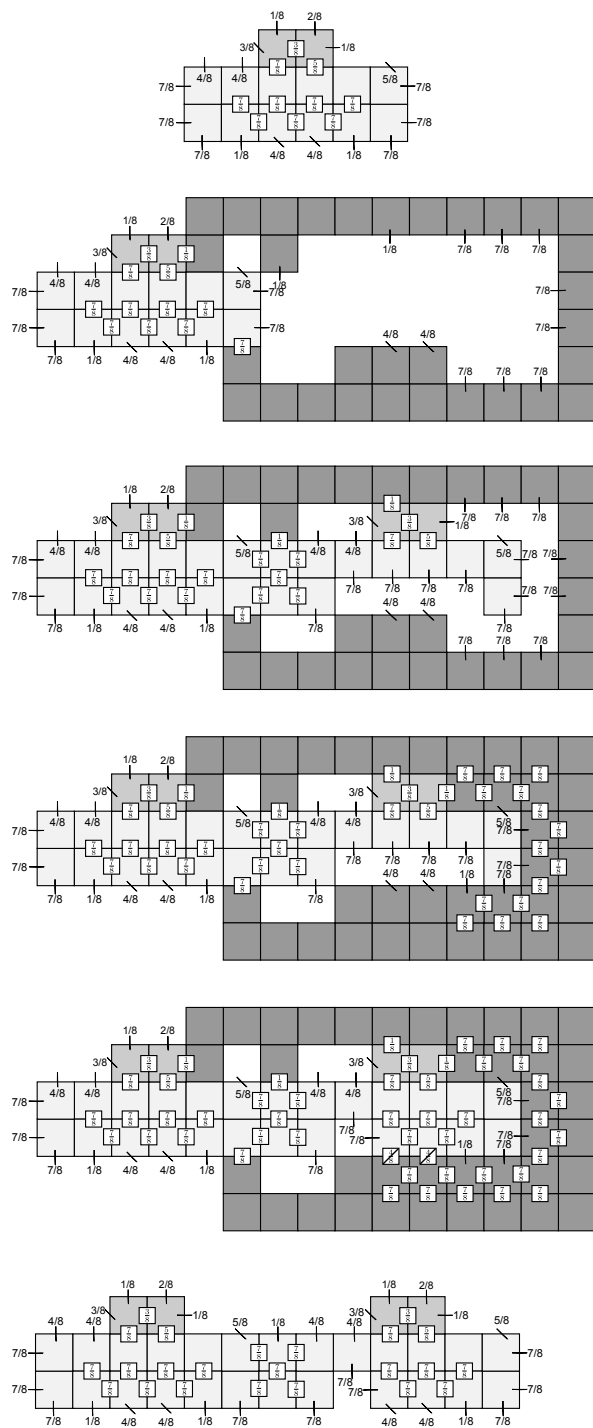


Figure 13: This figure shows the steps that occur when extending the tape to the right.

## 6 Future Work

The results of this paper raise a number of interesting research questions. The first focusses on the primary drawback of our technique: the use of negative strength glue interactions. Is fuel-efficient computation in passive self-assembly possible with the use of only positive strength glue interactions? Such a system seems difficult to imagine as positive strength systems may only grow and cannot break apart under current standard models. However, there is currently no proof that such a system cannot exist, even in very restricted settings such as the standard positive strength tile assembly model.

Another direction of research is the application of fuel-efficient constructions to complexity questions in tile self-assembly. For example, the existence of a space-efficient tile system with negative strength glues that simulates universal computation implies that some interesting verification problems in tile self-assembly become uncomputable. Does the existence of fuel-efficient systems have similar implications to computability and complexity?

An additional metric that tile assembly research often attempts to minimize is the *temperature* of the tile system. The temperature is an additional positive integer parameter included in a tile system that dictates how much glue strength is required for two assemblies to stick together. In our paper, if we restrict ourselves to integer glue strengths and include a temperature parameter, our constructions correspond to temperature 8 systems. An interesting question is to determine the smallest integer temperature value at which fuel-efficient computation can take place.

Another interesting general direction is to explore alternate fuel sources for tile assembly. In this paper we have focussed on the natural metric of permanent tile expenditure. An alternate approach is to consider some modification to the model that permits harnessing an external fuel source. One example is a self-assembly system in which the temperature of the system perpetually oscillates up and down. Is it possible to harness such oscillation to obtain a *fuel neutral* self-assembly system? Do there exist other promising and practically motivated fuel models, such as a model that incorporates a single type of active *fuel rod* component to fuel the assembly?

An additional promising direction is to explore the extent to which active behavior can be simulated within passive self-assembly models. One recent model of active self-assembly is the *signal tile assembly model* in which tiles may pass single, fire-once signals across tile faces. Such systems are known to

be capable of fuel-efficient computation. Can passive self-assembly tile systems with negative glue interactions simulate general signal tile systems?

Finally, while our construction fuel-efficiently simulates a single tape Turing machine, the question of fuel-efficient simulation of more efficient machines, such as a two-tape Turing machine, is still open. In particular, two-tape Turing machines are perhaps the “machine of choice” among Turing machine programmers. In addition, two-tape machines offer a linear factor efficiency improvement over single tape machines. Therefore, it is extremely interesting to know if it is possible to fuel-efficiently simulate a two-tape machine in passive self-assembly, or even in more active models of self-assembly.

### Acknowledgements

We would like to thank Damien Woods, Alexandra Keenan, Xingsi Zhong, Jennifer Padilla, Matt Patitz, Scott Summers, and Dave Doty for helpful discussions and comments during the writing of this paper. We would also like to thank the anonymous reviewers for their constructive feedback which has been incorporated into the paper.

### References

- [1] Zachary Abel, Nadia Benbernou, Mirela Damian, Erik Demaine, Martin Demaine, Robin Flatland, Scott Kominers, and Robert Schweller, *Shape replication through self-assembly and RNase enzymes*, SODA 2010: Proceedings of the Twenty-first Annual ACM-SIAM Symposium on Discrete Algorithms (Austin, Texas), Society for Industrial and Applied Mathematics, 2010.
- [2] Leonard Adleman, Qi Cheng, Ashish Goel, and Ming-Deh Huang, *Running time and program size for self-assembled squares*, Proceedings of the thirty-third annual ACM Symposium on Theory of Computing (New York, NY, USA), ACM, 2001, pp. 740–748.
- [3] Leonard Adleman, Qi Cheng, Ashish Goel, Ming-Deh Huang, and Hal Wasserman, *Linear self-assemblies: Equilibria, entropy and convergence rates*, In Sixth International Conference on Difference Equations and Applications, Taylor and Francis, 2001.
- [4] Leonard M. Adleman, Qi Cheng, Ashish Goel, Ming-Deh A. Huang, David Kempe, Pablo Moisset de Espanés, and Paul W. K. Rothmund, *Combinatorial optimization problems in self-assembly*, Proceedings of the Thirty-Fourth Annual ACM Symposium on Theory of Computing, 2002, pp. 23–32.
- [5] Leonard M. Adleman, Jarkko Kari, Lila Kari, Dustin Reishus, and Petr Sosík, *The undecidability of the infinite ribbon problem: Implications for computing by self-assembly*, SIAM Journal on Computing **38** (2009), no. 6, 2356–2381.
- [6] Gagan Aggarwal, Qi Cheng, Michael H. Goldwasser, Ming-Yang Kao, Pablo Moisset de Espanés, and Robert T. Schweller, *Complexities for generalized models of self-assembly*, SIAM Journal on Computing **34** (2005), 1493–1515, Preliminary version appeared in SODA 2004.
- [7] Robert D. Barish, Rebecca Schulman, Paul W. Rothmund, and Erik Winfree, *An information-bearing seed for nucleating algorithmic self-assembly*, Proceedings of the National Academy of Sciences **106** (2009), no. 15, 6054–6059.
- [8] Florent Becker, Ivan Rapaport, and Eric Rémila, *Self-assembling classes of shapes with a minimum number of tiles, and in optimal time*, Foundations of Software Technology and Theoretical Computer Science (FSTTCS), 2006, pp. 45–56.
- [9] Nathaniel Bryans, Ehsan Chiniforooshan, David Doty, Lila Kari, and Shinnosuke Seki, *The power of nondeterminism in self-assembly*, SODA 2011: Proceedings of the 22nd Annual ACM-SIAM Symposium on Discrete Algorithms, SIAM, 2011, pp. 590–602.
- [10] Sarah Cannon, Erik D. Demaine, Martin L. Demaine, Sarah Eisenstat, Matthew J. Patitz, Robert Schweller, Scott M. Summers, and Andrew Winslow, *Two hands are better than one (up to constant factors)*, Arxiv preprint arXiv:1201.1650 (2012).
- [11] Harish Chandran, Nikhil Gopalkrishnan, and John H. Reif, *The tile complexity of linear assemblies*, 36th International Colloquium on Automata, Languages and Programming, vol. 5555, 2009.
- [12] Ho-Lin Chen and David Doty, *Parallelism and time in hierarchical self-assembly*, SODA 2012: Proceedings of the 23rd Annual ACM-SIAM Symposium on Discrete Algorithms, SIAM, 2012.
- [13] Ho-Lin Chen, David Doty, and Shinnosuke Seki, *Program size and temperature in self-assembly*, ISAAC 2011: Proceedings of the 22nd International Symposium on Algorithms and Computation, Lecture Notes in Computer Science, vol. 7074, Springer-Verlag, 2011, pp. 445–453.
- [14] Matthew Cook, Yunhui Fu, and Robert T. Schweller, *Temperature 1 self-assembly: Deterministic assembly in 3d and probabilistic assembly in 2d*, SODA, 2011, pp. 570–589.
- [15] Nadine Dabby and Ho-Lin Chen, *Active self-assembly of simple units using an insertion primitive*, SODA 2013: Proceedings of the Twenty-fourth Annual ACM-SIAM Symposium on Discrete Algorithms, 2013.
- [16] Erik D. Demaine, Martin L. Demaine, Sándor P. Fekete, Mashhood Ishaque, Eynat Rafalin,

- Robert T. Schweller, and Diane L. Souvaine, *Staged self-assembly: nanomanufacture of arbitrary shapes with  $O(1)$  glues*, *Natural Computing* **7** (2008), no. 3, 347–370.
- [17] Erik D. Demaine, Sarah Eisenstat, Mashhood Ishaque, and Andrew Winslow, *One-dimensional staged self-assembly*, Proceedings of the 17th international conference on DNA computing and molecular programming, DNA'11, 2011, pp. 100–114.
- [18] Erik D. Demaine, Matthew J. Patitz, Robert T. Schweller, and Scott M. Summers, *Self-assembly of arbitrary shapes using RNase enzymes: Meeting the Kolmogorov bound with small scale factor*, STACS 2011: Proceedings of the 28th International Symposium on Theoretical Aspects of Computer Science, 2011.
- [19] David Doty, *Randomized self-assembly for exact shapes*, *SIAM Journal on Computing*, to appear.
- [20] David Doty, Lila Kari, and Benoît Masson, *Negative interactions in irreversible self-assembly*, DNA 16: Proceedings of The Sixteenth International Meeting on DNA Computing and Molecular Programming, Lecture Notes in Computer Science, Springer, 2010, pp. 37–48.
- [21] David Doty, Jack H. Lutz, Matthew J. Patitz, Robert Schweller, Scott M. Summers, and Damien Woods, *The tile assembly model is intrinsically universal*, FOCS 2012: Proceedings of the 53rd IEEE Conference on Foundations of Computer Science, 2012.
- [22] David Doty, Matthew J. Patitz, Dustin Reishus, Robert T. Schweller, and Scott M. Summers, *Strong fault-tolerance for self-assembly with fuzzy temperature*, FOCS 2010: Proceedings of the 51st Annual IEEE Symposium on Foundations of Computer Science, IEEE, 2010, pp. 417–426.
- [23] Bin Fu, Matthew J. Patitz, Robert Schweller, and Robert Sheline, *Self-assembly with geometric tiles*, ICALP 2012: Proceedings of the 39th International Colloquium on Automata, Languages and Programming (Warwick, UK), 2012.
- [24] Kenichi Fujibayashi, Rizal Hariadi, Sung Ha Park, Erik Winfree, and Satoshi Murata, *Toward reliable algorithmic self-assembly of dna tiles: A fixed-width cellular automaton pattern nano letters*, (2007).
- [25] Ming-Yang Kao and Robert T. Schweller, *Reducing tile complexity for self-assembly through temperature programming*, SODA 2006: Proceedings of the 17th Annual ACM-SIAM Symposium on Discrete Algorithms, 2006, pp. 571–580.
- [26] ———, *Randomized self-assembly for approximate shapes*, International Colloquium on Automata, Languages, and Programming, Lecture Notes in Computer Science, vol. 5125, Springer, 2008, pp. 370–384.
- [27] Ján Maňuch, Ladislav Stacho, and Christine Stoll, *Step-assembly with a constant number of tile types*, ISAAC 2009: Proceedings of the 20th International Symposium on Algorithms and Computation (Berlin, Heidelberg), Springer-Verlag, 2009, pp. 954–963.
- [28] Jennifer E. Padilla, Matthew J. Patitz, Raul Pena, Robert T. Schweller, Nadrian C. Seeman, Robert Sheline, Scott M. Summers, and Xingsi Zhong, *Asynchronous signal passing for tile self-assembly: Fuel efficient computation and efficient assembly of shapes*, Arxiv preprint arXiv:1202.5012 (2012).
- [29] Matthew J. Patitz, Robert T. Schweller, and Scott M. Summers, *Exact shapes and turing universality at temperature 1 with a single negative glue*, Proceedings of the Seventeenth International Conference on DNA Computing and Molecular Programming (DNA 17) (California Institute of Technology, Pasadena, CA), 2011.
- [30] Paul W.K. Rothemund, Nick Papadakis, and Erik Winfree, *Algorithmic self-assembly of DNA Sierpinski triangles*, *PLoS Biology* **2** (2004), no. 12, 2041–2053.
- [31] David Soloveichik and Erik Winfree, *Complexity of self-assembled shapes*, *SIAM Journal on Computing* **36** (2007), no. 6, 1544–1569.
- [32] Scott M. Summers, *Reducing tile complexity for the self-assembly of scaled shapes through temperature programming*, *Algorithmica* **63** (2012), no. 1, 117–136.
- [33] Erik Winfree, *Algorithmic self-assembly of DNA*, Ph.D. thesis, California Institute of Technology, June 1998.
- [34] Damien Woods, Ho-Lin Chen, Scott Goodfriend, Nadine Dabby, Erik Winfree, and Peng Yin, *Efficient active self-assembly of shapes*, Manuscript (2012).